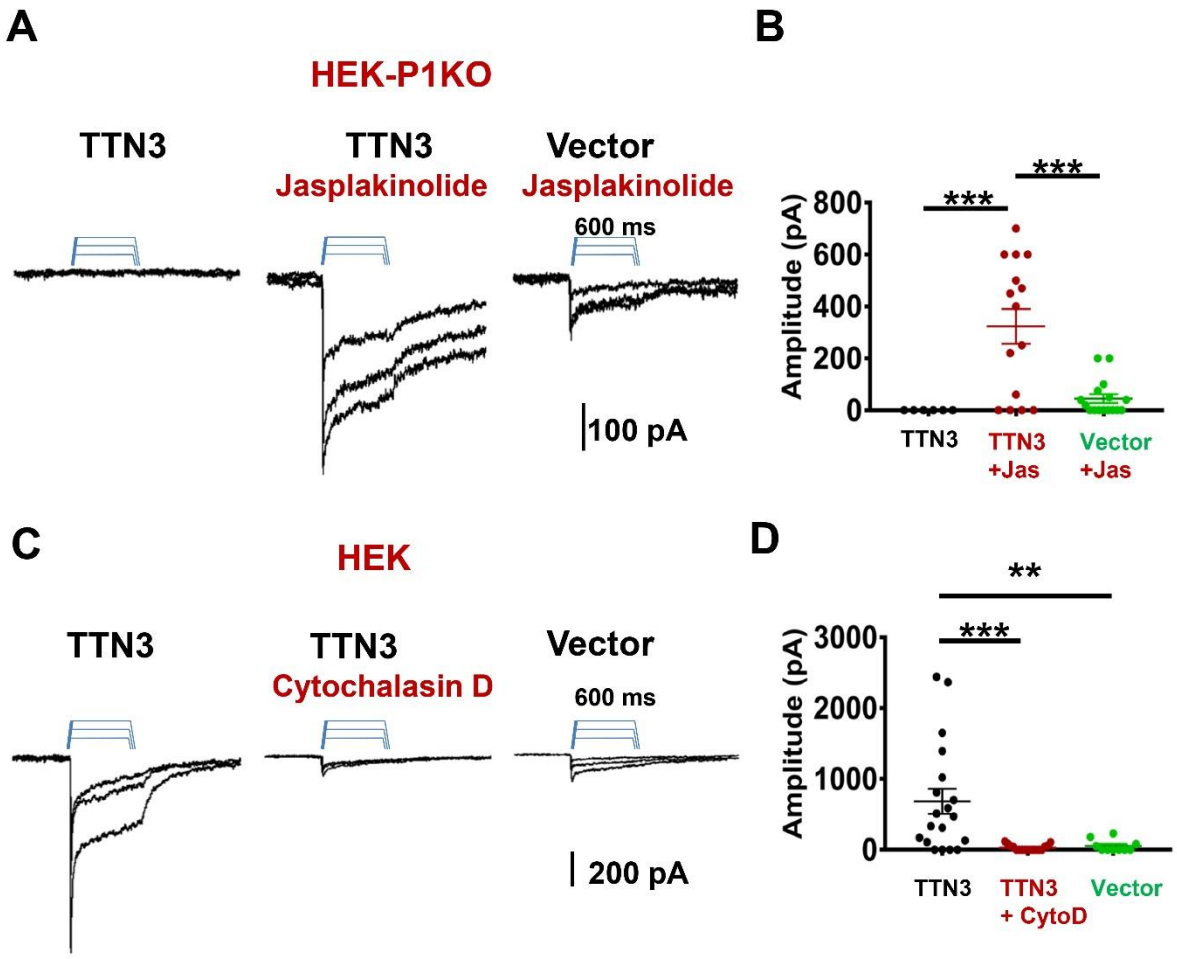

Supplemental Figure 1. Mechanically-activated currents in *Ttn3*-transfected *Piezo1*-knock out HEK cells after incubation with jasplakinolide.

(A) Representative traces of mechanically-activated (MA) currents activated by mechanical step stimuli in *Ttn3*-transfected *Piezo1*-knock out HEK (HEK-P1KO) cells (left), *Ttn3*- or vector-transfected HEK-P1KO cells pretreated with 250 nM jasplakinolide for two hrs.

(B) Average peak amplitudes of MA currents activated by a 5-μm mechanical step in *Ttn3*-transfected HEK-P1KO cells (TTN3, n = 6), *Ttn3*- (n = 15) or vector-transfected (n = 16) HEK-P1KO cells pretreated with 250 nM jasplakinolide for two hrs (TTN3+Jas and Vector+Jas, respectively). Data represent mean ± SEM. ***P < 0.001 by one-way ANOVA with Dunnett's post hoc test).

(C) Representative traces of MA currents in HEK cells transfected with *Ttn3* without (left) and with 5 μM cytochalasin D treatment (middle). MA currents in HEK cells transfected with a vector plasmid were also shown for control (right).

(D) Average peak amplitudes of MA currents activated by a 5-μm mechanical step in *Ttn3*-transfected HEK cells without (n = 19) or with cytochalasin D (n = 17) and vector-transfected HEK cells (n = 10). Data represent mean ± SEM. **P < 0.01, ***P < 0.001 by one-way ANOVA with Dunnett's post hoc test.

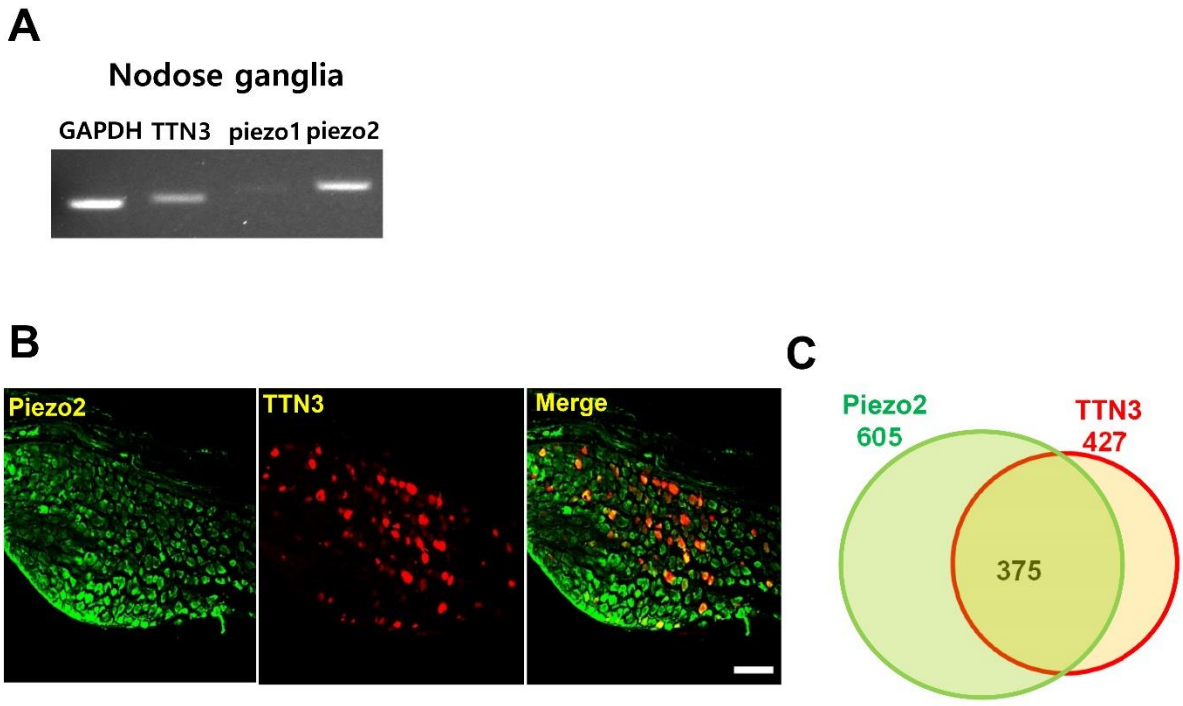

Supplemental Figure 2. Colocalization of TTN3 with Piezo2 in NG neurons.

(A) RT-PCR analysis showing expressions of TTN3, Piezo1 and Piezo2 in nodose ganglia.

(B) Immunofluorescence images showing the colocalization of TTN3 with Piezo2. mCherry was expressed in TTN3-positive NG neurons after AAVDJ-EF1a-DIO-mCherry infection to the nodose ganglia of *Ttn3*^{Cre} mice. Scale bar represents 100 μm.

(C) A Venn diagram illustrating the proportion of colocalization of TTN3 and Piezo2 in NG neurons (n= 3 mice). Numbers represent the number of TTN3 and/or Piezo2 expressing NG cells.

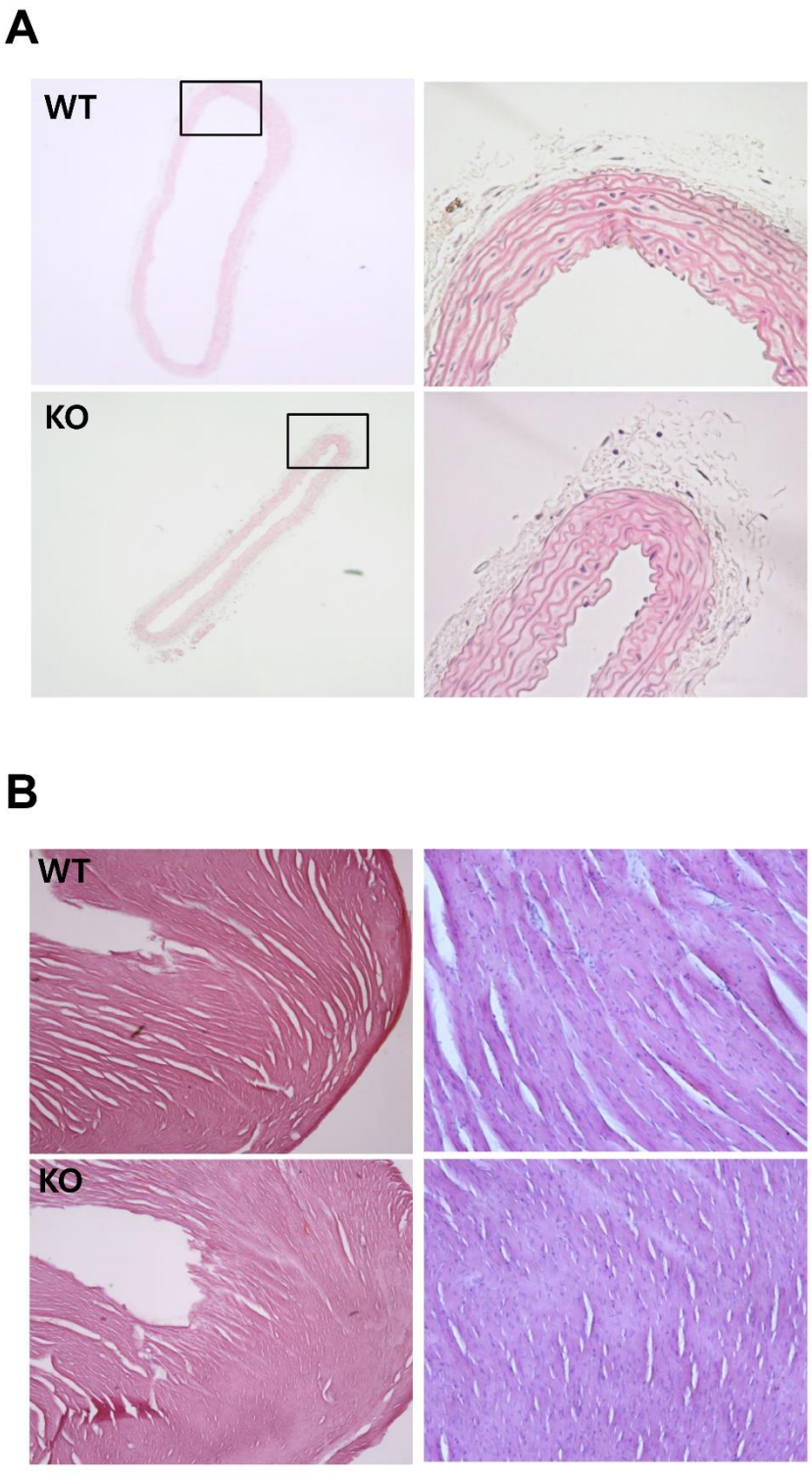

Supplemental Figure 3. Hematoxilin & eosin staining of the aorta (A) and left ventricle of the heart (B) of WT and *Ttn3*$^{-/-}$ mice. Images in the right panels of (A) are magnified images in the box in the left panels. Note that overall structures of the aorta and myocardium of both genotypes are comparable.

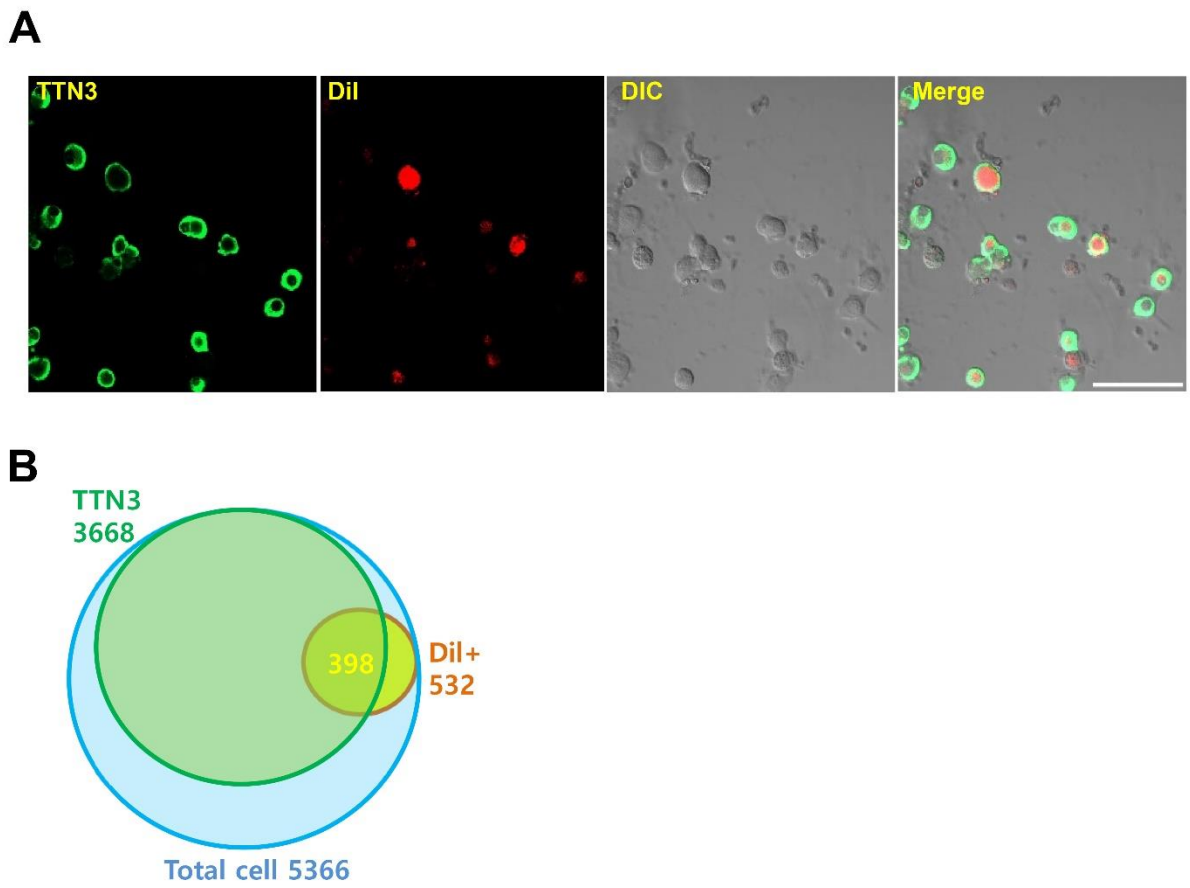

Supplemental Figure 4. TTN3-positive neurons project to aortic arch.

(A) Immunofluorescent images of TTN3- and/or DiI-positive NG neurons isolated from nodose-ganglia of WT mice. DiI was injected into the aortic arch 7 days prior to the isolation of nodose ganglia. Scale bar represents 100 μm.

(B) A Venn diagram illustrating the proportion of TTN3- and/or DiI-positive NG neurons (n = 3 mice).

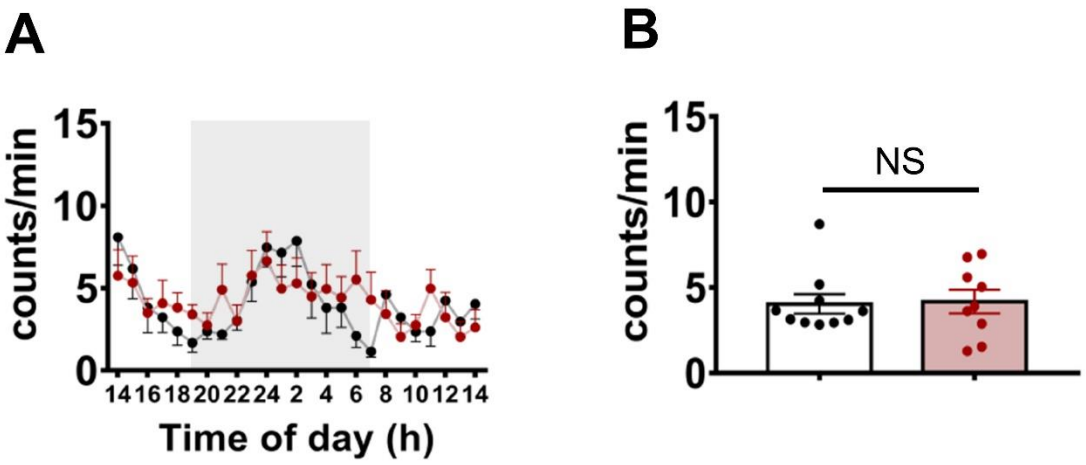

Supplemental Figure 5. Motor activity of WT and TTN3$^{-/-}$ mice.

(A) Motor activities of WT (black, n = 10) and *Ttn3*$^{-/-}$ mice (Red, n = 9) recorded for 24 h. Data represent mean ± SEM.

(B) Summary of average motor activities in 24 h of both genotypes. Data represent mean ± SEM. NS, not significant.

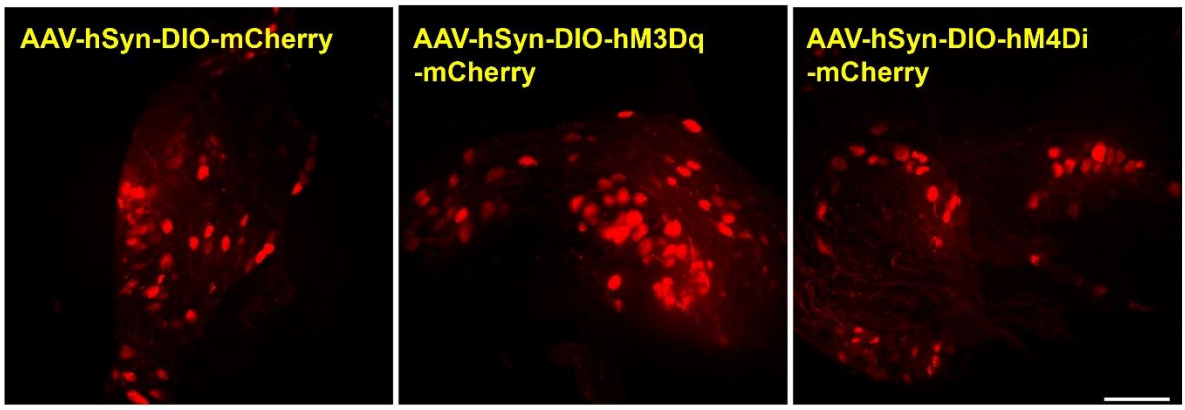

Supplemental Figure 6. mCherry expression in NG neurons after the infection of AAV-hSyn-DIO-mCherry, AAV-hSyn-DIO-*hM3Dq*-mCherry, or AAV-hSyn-DIO-*hM4Di*-mCherry infection into nodose ganglia of TTN3^{cre} mice. Scale bar represents 100 μm.